ADVANCED MATERIALS

DOI: 10.1002/adma.200701428

Surface Nanopatterning to Control Cell Growth**

By *Ludovic Richert, Fiorenzo Vetrone, Ji-Hyun Yi, Sylvia Francis Zalzal, James D. Wuest, Federico Rosei,* and *Antonio Nanci**

A significant challenge in implantology is the design of biomaterials that actively promote functional regeneration of the host tissue while avoiding undesirable tissue responses. This requires selective control of interactions at the tissue/implant interface, the site of a series of complex events that depend on synergistic parameters including surface chemistry,[1] elasticity,[2] topography,[3] and energy.[4] To date, efforts have focused largely on defining how microtexture influences the molecular and cellular events of tissue repair.[5] However, it is now widely recognized that biological substrates on which cells thrive consist of nanostructured molecular networks, and the sensing apparatus of cells operates on the nanometer scale. Reports have emerged showing that nanometer-scale surface features can influence cellular attachment, differentiation, and alignment.[6–9] The present study takes an important further step by showing how simple chemical treatment can generate multifunctional nanostructured surfaces that control cell growth selectively. These surfaces promote the growth of certain cells while inhibiting that of others, without the addition of any exogenous biological or pharmacological agents.

Cellular response to the surface features in the micrometer-range such as grooves, ridges, and wells has been well established.[10–12] In the past few years, interest has shifted to evaluating the potential of nanostructured biomaterials for affecting cellular activity.[9,13,14] Work in this area has been facilitated by recent advances in technologies used to modify and observe surfaces with nanostructural features.[9] Nanostructural features for biological interfaces can be created by various techniques such as photolithography,[12] deposition of particles,[15] polymer demixing,[9,16] and metal evaporation.[6] These approaches can yield uniform arrays of various types, including troughs, grooves, and protrusions with nanometer-scale dimensions. We have also previously shown that chemical treatment with a mixture of H_2SO_4/H_2O_2 can uniquely generate spongelike networks of nanopits within the surface layer of titanium-based metals.[17] These nanoporous surfaces promote both early and longer-term osteogenic events in cell cultures, thereby imparting bioactive properties to the materials.[18,19] These intriguing results led us to study in detail how the nanoporous surfaces are created and how they affect various cell types. Here, we have focused on the use of H_2SO_4/H_2O_2 and have examined the effects of experimental conditions with two goals in mind: (1) to modulate the formation of nanopores on titanium alloy (Ti6Al4V), and (2) to thereby control the growth of common cell types on this widely used implant metal. Osteogenic cells were evaluated because they are critical for the successful integration of implants in bone. Fibroblastic cell lines were studied because formation of a fibrous capsule weakens the bone/implant interface and represents a major complication for permanent implants, ultimately requiring their replacement. Smooth muscle cells (SMC) were investigated because their hypertrophy and proliferation are widely known to contribute to the restenosis of blood vessels after corrective surgery.[20] In all cases, culture intervals corresponding to initial stages of cell colonization were examined, as these are critical for biomaterial integration at any site of implantation.

By simply immersing titanium alloy disks in a mixture consisting of a strong acid (H_2SO_4, sulfuric acid) and an oxidant (H_2O_2, hydrogen peroxide), it was possible to create a reproducible spongelike network of nanopits on their surface. The rationale for using such a mixture to nanotexture metals was to first etch the surface with an acid and then reoxidize it in a controlled manner.[17] Our methodology proved to generate a range of micro- and nanotopographies. When analyzed by scanning electron microscopy (SEM) at low magnification, the machined metal surfaces of untreated controls, polished to a mirror finish, exhibited only shallow grooves resulting from the machining process (Fig. 1a). Moreover, at high magnification, they did not reveal any nanotopographical features (Fig. 1b). Micrometer-scale images obtained by atomic force microscopy (AFM) showed only attenuated marks, and nanometer-scale images revealed a slight undulating pattern but no nanotopographical features (Fig. S1).

[*] Prof. A. Nanci, Dr. L. Richert, Dr. J.-H. Yi, S. F. Zalzal
Laboratory for the Study of Calcified Tissues & Biomaterials
Faculté de Médecine Dentaire, Université de Montréal
Montréal, QC, H3T 1J4 (Canada)
E-mail: antonio.nanci@umontreal.ca
Dr. F. Vetrone, Prof. F. Rosei
Institut National de la Recherche Scientifique-Énergie
Matériaux et Télécommunications, Université du Québec
1650, boul. Lionel-Boulet, Varennes, QC J3X 1S2 (Canada)
Prof. J. D.Wuest
Département de Chimie, Université de Montréal
Montréal, QC, H3T 1J4 (Canada)

[**] We acknowledge funding from the Canadian Institutes of Health Research (CIHR) and the Natural Sciences and Engineering Research Council of Canada (NSERC) through a Collaborative Health Research Project. A.N. also acknowledges funding from the CIHR and the Canada Foundation for Innovation (CFI). F.R. is grateful to Fonds quebecois de recherches sur la nature et les technologies (FQRNT) and for start-up funds from INRS. F.R. and J.D.W. acknowledge support from the Canada Research Chairs Program and from NSERC (Discovery Grants). F.V. is grateful for a postdoctoral fellowship from NSERC and L.R. for a postdoctoral fellowship from Fonds de la Recherche en Santé du Quebec (FRSQ). Supporting Information is available online from Wiley InterScience or from the authors.

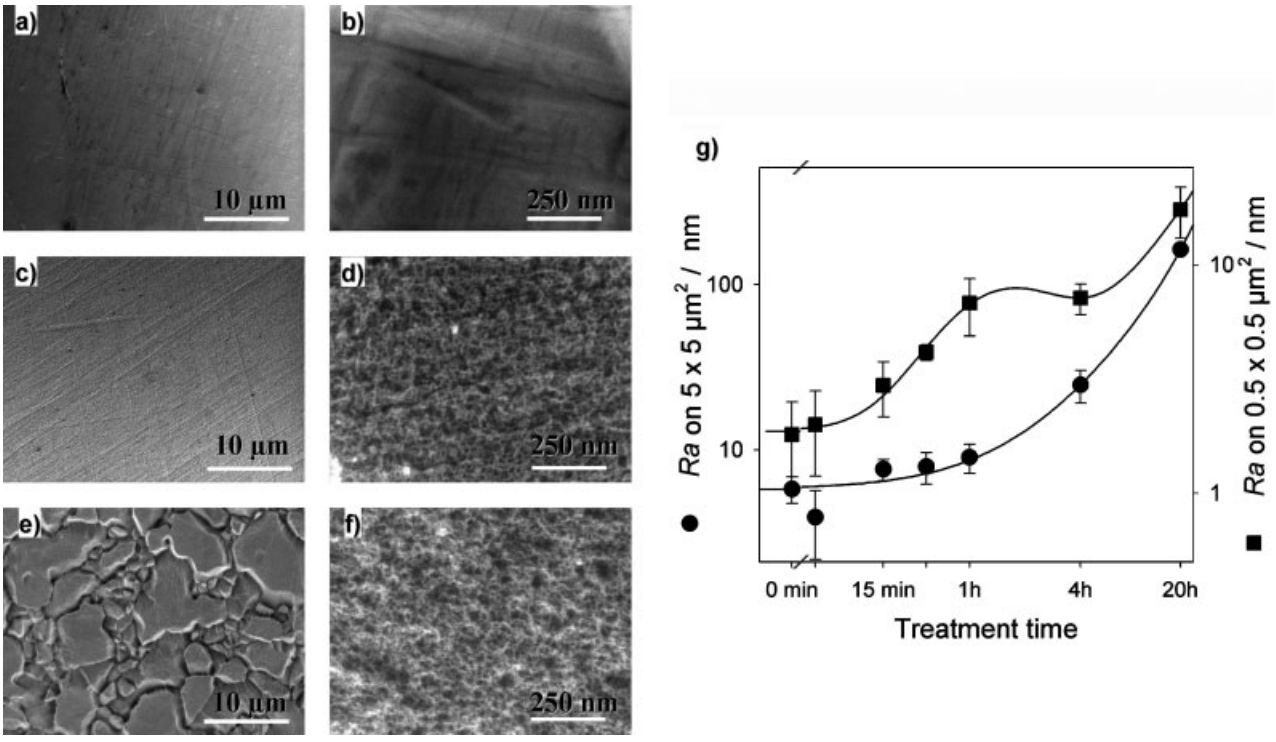

Figure 1. a)–f). Scanning electron micrographs showing low-resolution (a, c, e) and high-resolution images (b, d, f) of untreated (a, b) polished Ti6Al4V surfaces, and surfaces following exposure to H_2O_2/H_2SO_4 for 1 h (c, d) and 20 h (e, f). (Images of surfaces obtained with other times of treatment are presented as Supporting Information.) Figure (g) is a graph showing the evolution of average roughness (Ra) of the surface during treatment measured with AFM (tapping mode) on $5 \times 5\ \mu m^2$ (●) and on $0.5 \times 0.5\ \mu m^2$.

After 1 h of immersion in the etching mixture at 21 °C, the surface of titanium alloy disks remained relatively smooth on the micrometer scale (Fig. 1c). However, the controlled chemical oxidation created a reproducible nanotexture involving the progressive generation of nanopits, which changed structurally with increasing treatment time. At treatment times longer than 1 h, the formation of microtexture was found to begin with an attack at the grain boundaries (Fig. 1e), and after 4 h the new texture had become quite noticeable (Supporting Information Figs. S1 and S2). The nanotexture appeared during the first hour, leading to an increase in roughness by a factor of 4 at the nanometer scale with respect to the untreated disks (control). Thereafter, the nanopits continued to evolve (Fig. 1d and f, Tables 1 and S1).

After 20 h of treatment, the microtexture was well-established, clearly exhibiting the protrusion of the larger grains. Elemental analysis (by energy-dispersive X-ray analysis) showed that grains rich in vanadium (β grains) are more strongly affected by

Table 1. Summary of the texture and cellular growth on Ti6Al4V for the major times of treatment (data for intermediate times (5 min, 30 min, 4 h) and statistical analyses are presented as Supporting Information).

Treatment time		0 (control)	1 h	20 h
Surface aspect		Mirror	Gold mirror	Matte gray
Nanotexture		No	Yes	Yes
Microtexture		No	No	Yes
Nanopore size [nm]		N/A	23 ± 6.9	32.8 ± 11.9
Contact angle [water, 30 s]		$51° \pm 9.7°$	$35° \pm 1.9°$	$32° \pm 2.5°$
Roughness [nm]	$5 \times 5\ \mu m^2$	5.8 ± 1.0	9.0 ± 2.4[a]	163 ± 7.8[a]
	$0.5 \times 0.5\ \mu m^2$	1.8 ± 0.7[a]	7.2 ± 2.4[a]	17 ± 4.4[a]
Cell adhesion after 6 h[b]	Smooth muscle cells	100 ± 21	92 ± 14	97 ± 19
	Osteoblasts	100 ± 26	137 ± 11	120 ± 11
	Fibroblasts	100 ± 27	95 ± 10	111 ± 23
	Smooth muscle cells	5.22 ± 0.43	6.08 ± 0.55	5.19 ± 0.66
Cell growth [c]	Osteoblasts	1.46 ± 1.04	4.32 ± 0.27	1.78 ± 0.51
	Fibroblasts	3.84 ± 0.54	2.24 ± 0.51[a]	1.62 ± 0.49

[a]$p < 0.05$. [b]Control: 100. [c]Ratio of cell count at 3 days to cell count at 6 h.

ADVANCED MATERIALS

chemical treatment (Fig. S3, Table S4). The surface roughness attained a value 20 times higher than that observed after only 1 h of treatment (Figs. 1g and S1, Table 1). While preferential attack at grain boundaries may affect mechanical properties, a recent study in which H_2SO_4 was used for anodization of a titanium alloy (Ti6Al7Nb) demonstrated that selective etching of grains and nanometer-scale surface modifications do not affect the mechanical properties.[21] The diameter of nanopits likewise increased from approximately 23 nm (after 1 h of treatment) to 32 nm (after 20 h), a 35% increase (Fig. 1g, Table 1). These results suggest that microtexture and nanotexture created by chemical treatment with H_2SO_4/H_2O_2 proceed with different kinetics and involve different mechanisms. Contact angle measurements (Table 1) indicated that longer treatments led to a moderate increase in hydrophilicity, which becomes more accentuated with the development of microtexture.

To determine the influence of the nanoporosity created by H_2SO_4/H_2O_2 treatment on cellular growth, we measured cell adhesion and short-term cell growth for three different cell lines. The counts obtained revealed that the three cell types examined respond differently to nanostructured Ti6Al4V (Fig. 2).

Growth of the A7r5 SMC line was not significantly affected by the microtexture, the range of nanopores, and the surface roughness we have generated (Fig. 2a). Thapa et al.[22] have shown that nanotextured surfaces can promote both adhesion and growth of SMC, as well as adhesion of bladder smooth muscle cells. However, both the material and surface structures examined by these investigators differed substantially from ours. They used chemical treatment to achieve nanoscale surface protrusions on biodegradable polymers, and they concluded that the observed effects resulted primarily from surface roughness. Their best results were obtained at a roughness superior to 200 nm, whereas the maximum roughness achieved in our study was substantially below this value (Fig. 1g).

After 6 h, the number of fibroblastic cells on treated surfaces proved to be similar to that on controls, but after 3 days of growth the number was significantly lower (Fig. 2b). This indicates that the nanotexture generated by treatment with H_2SO_4/H_2O_2 has no effect on the adhesion of fibroblastic cells but in fact limits their growth, a finding which differs from data showing that surfaces with nanoscale islands stimulate fibroblast activity.[23] This striking effect resulting from our treatment suggests that nanotextured surfaces can be used to limit the growth of fibroblasts and can thereby retard the undesirable formation of fibrous capsules around implants.

Cell counts at 3 days showed that treatment with H_2SO_4/H_2O_2 promotes the growth of osteogenic cells, with the strongest effect seen after 1 h of treatment (Fig. 2c). As the treatment time was lengthened, the resulting increase in microscale surface roughness limited cell growth. The inhibitory influence of microtexture was most evident on surfaces treated for 20 h; at this point, the benefits of nanotopography were cancelled by microroughness, and cell density returned to the levels of controls at early culture intervals. The inhibitory effect of microroughness is consistent with the findings of Anseleme and Bigerelle,[24] who have shown that the beneficial influence of microtopography on osteogenic cell activity actually results from chemical modification of the surface rather than topographic cuing. Alternatively, microroughness may cause a differential adsorption of proteins such as albumin and fibronectin which has been shown to influence the response of bone marrow cells on Ti6Al4V.[25]

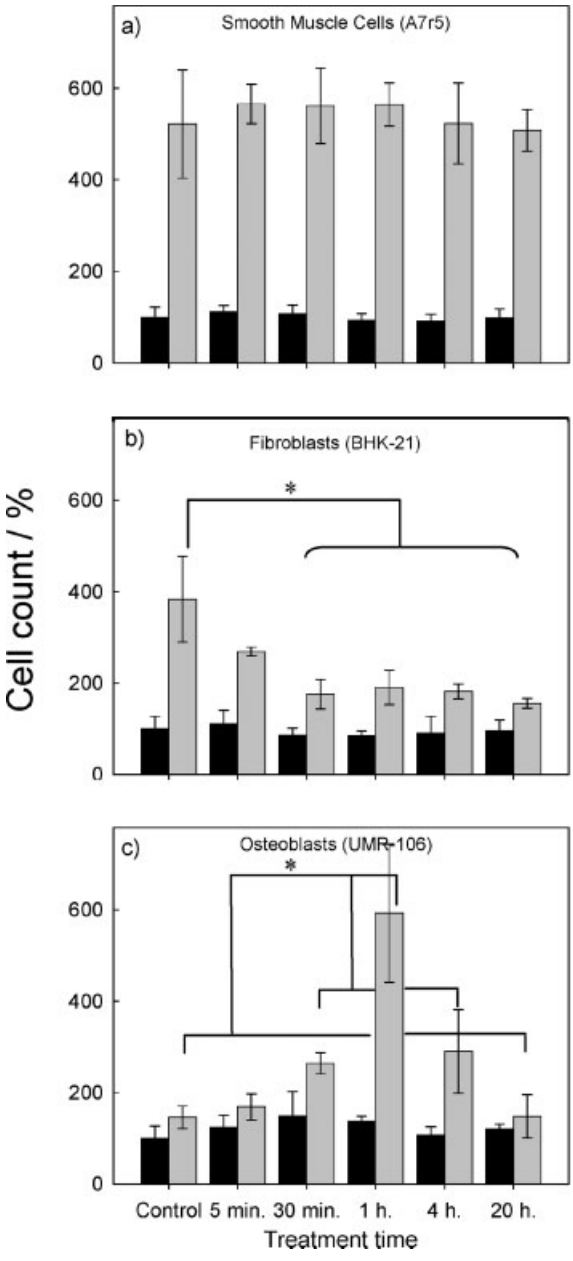

Figure 2. Evaluation of cell count by light microscopy (objective 10 X) after 6 h (black bar) and 3 days (gray bar) on different treated Ti6Al4V substrates (and control) for three different cell lines: smooth muscle cells (SMC) (a), fibroblasts (b), and osteoblasts (c) expressed as % of control count at 6 h (* $p < 0.05$)

The stimulatory effect on osteogenic cells achieved with 1 h of treatment by H_2SO_4/H_2O_2 was also validated by examining the growth of primary rat calvaria-derived osteogenic cells on Ti6Al4V disks in which only half the surface was treated. This protocol had the distinct advantage of permitting an evaluation of how the same population of cells simultaneously responds to both native and nanotextured surfaces in the absence of microtexture. After 3 days of culture, more cells were observed on the nanostructured half of the disk [around 50% ($p < 0.05$)]. Furthermore, the cells were also more widely spread on the nanotextured surface, where they occupied ~80% ($p < 0.05$) more surface than on the controls (Fig. 3). These results are consistent with data obtained with transformed osteogenic cell lines and with previous reports that osteogenic cells are positively influenced by nanotopography,[26–28] and promote formation of bone-like nodules.[19]

It is now increasingly recognized that cells are governed in part by the same nanoscale architectural features that control non-biological phenomena at interfaces, reaffirming the importance of integrating physics and biology. Our observations are distinctive and significant because they demonstrate that simple methods can be used to generate nanostructured surfaces that promote the growth of osteoblasts, while at the same time limiting that of fibroblastic cells. This is the first time that a nanostructured metal surface created by oxidative patterning has been shown to have a differential effect. Although it cannot be excluded that some of the observed effects on cell activity after 1 hour of treatment may in part be due to microroughness, such a contribution is unlikely or would be minor for the following reasons: (1) the increase in microroughness is very small compared to control values and measures in nm, (2) it is not in the range reported to influence cell activity,[11,24,29] and (3) when the increase is more significant (e.g., 20 h treatment), it actually limits osteogenic cell growth. The wetting angle is also a key parameter for cell adhesion and proliferation, but it should be noted that the contact angles always remain below 60° across the various surface treatment times. Such values are not considered sufficient to alter cellular activity significantly.[4] The differential effect observed on the 3 cell types tested also raises questions about the impact of wetting angle. However, it should be noted that for the fibroblastic cells there is a similarity between the contact angle values and the trend in cell counts at 6 h (cell adhesion) (Table S1). Finally, while between 30 min and 1h changes in microroughness and contact angle are negligible, there is a significant increase in osteoblastic cell counts at 3 days (cell growth) (Table S1).

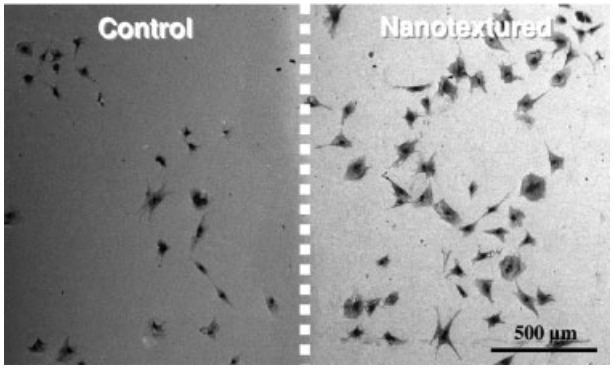

Figure 3. Comparative SEM images of primary osteoblasts after 3 days of culture on smooth (left) and nanotextured (right) portions of a Ti6Al4V disk. Side-by-side surfaces were obtained by treating only half of the disk for 1 hour.

Knowledge of how the topography of an implant surface promotes or impedes a specific cellular recolonization is needed to design novel surfaces that can sustain and improve tissue repair. Although there has been much interest in modulating cell adhesion for improving colonization of biomaterial surfaces, we have shown that oxidative nanopatterning can achieve the same outcome by favoring cellular growth instead. It is noteworthy that the dimensions, structural organization, and roughness of the nanoporous networks we have generated bear resemblance to the supramolecular organization of extracellular matrix proteins such as fibrinogen, collagen, and basement membrane constituents on which cells grow and thrive.[28,30,31] It is also possible that nanotextured surfaces adsorb proteins with preferential conformations and/or that they exhibit selective affinities for molecules that influence cell growth.[32,33]

In summary, by a simple controlled chemical oxidation of Ti6Al4V, we can obtain a network of nanopits, with or without a superimposed microtopography. The creation of these two levels of surface structuring appears to follow different kinetics, which could yield varied surface topographies capable of manipulating the growth of cells from different tissues. We believe that the nanoporous network signals cells directly by offering physical cues that are in the range of the cellular sensing apparatus. The precise mechanisms by which cells detect and respond to nanofeatures remain to be defined. It has been proposed that nanotopography may modulate cytoskeletal organization and membrane receptor organization.[14,28,31] The interaction of cells with the walls of the nanopits may cause sufficient local biomechanical deformation to activate specific signaling cascades that regulate cellular growth and eventually differentiation. Micro- and nanostructured surfaces may serve for various purposes, such as controlling and guiding cellular recolonization in the host by inducing osteogenesis and by suppressing the formation of fibrous tissue. Future work will focus on developing chemical treatments that can generate surfaces with a range of pore sizes mimicking more closely the various biological interfaces found in the body, and the effect on others cell types (HUVEC, macrophages, photoreceptor and stem cells) will be studied. Ultimately, it should be possible to generate surfaces that attract and guide the differentiation of stem cells *ex vivo* or *in vivo* along selected pathways without any addition of growth factors or signaling molecules. The rational design of such innovative biomaterials will require a profound understanding of their physicochemical characteristics and a close correlation with cell signaling mechanisms and molecular cascades.

ADVANCED MATERIALS

Experimental

Substrates and Surface Treatments: Ti6Al4V disks (14 mm in diameter and 2 mm in thickness) with a polished surface (generously supplied by DePuy Inc.) were washed with toluene (under sonication) and air dried. Controlled chemical oxidation resulting in a nanotextured surface was performed by exposing the disks to a solution consisting of equal volumes of H_2SO_4 (10 N) and aqueous H_2O_2 (30%) for various times at room temperature. Control substrates (non-treated disks) and treated disks were washed three times with deionized water, dried, and stored in a desiccator. For experiments with rat calvaria osteogenic cells, half the disk was protected with paraffin (Denco) before treatment for 1 h. The half-protected disk was then washed with water, paraffin was removed by washing in toluene, and the disk was washed with deionized water and similarly stored.

Surface Characterization: The surfaces of control and nanotextured disks were examined using a JEOL JSM-7400F field-emission scanning electron microscope operated at 1–2 kV. Surface roughness of the substrates was estimated by atomic force microscopy using a JEOL JSPM-5200 scanning probe microscope. Measurements were conducted in ambient air in tapping mode with ultra-sharp probes (SSS-NCHR, Nanosensors). The roughness values in the form of roughness average (Ra) were estimated with WinSPM (JEOL) on 0.5×0.5 and 5×5 μm^2 areas to obtain nanometric and micrometric information, respectively. Contact angles were obtained using the sessile drop method [34]. Images of drops (10 μL of 18.2 $M\Omega \cdot cm^{-1}$ water) were recorded with a contact angle goniometer NRL-100 (Ramé-Hart) after 30 s. The images were then analyzed by ImageJ (NIH) in conjunction with the Drop Shape plug-in (EPFL). This system measures the contact angle from the shape of the drop.

Cell Cultures: Smooth muscle cells (A7r5, CRL-1444, American Type Culture Collection (ATCC), fibroblasts (BHK-21, CCL-10, ATCC), osteoblasts (UMR-106, CRL-1661, ATCC), and primary rat calvaria osteogenic cells [19, 35] were used for the cell culture experiments. Disks were washed in pure ethanol, placed in 24-well cell culture plates, and exposed for a minimum of 15 min to UV light. Before cells were added, the disks were rinsed twice with sterile phosphate buffer saline (PBS) (15 min) and culture media without serum. Cells were cultured at a density of 10^4 cell/cm^2 under standard conditions (37 °C, 5% CO_2) in Dulbecco's Modified Eagle's Medium for A7r5 and α-Minimum Essential Medium for BHK-21, primary osteoblasts and UMR-106, both supplemented with fetal bovine serum (10%, FBS, Invitrogen) and penicillin/streptomycin (100 U mL^{-1}, Invitrogen). The medium was changed after two days during the studies.

At the end of the culture interval, the disks were rinsed three times with PBS, and cells were fixed with paraformaldehyde solution (4%) in PBS and stained with Hoechst 33258 (Sigma). The cell numbers were counted in three random fields per substrate with the aid of an epifluorescence microscope (Zeiss) with objective 10X. Cellular adhesion was evaluated by counting cells at 6 h, while counts at 3 days were used for cellular growth. The counts were expressed as cellular density normalized to 100 for the control, and the data were analyzed using the software "Rgui" (R Foundation for Statistical Computing).

Received: June 14, 2007
Revised: October 15, 2007
Published online: April 1, 2008

[1] S. Margel, E. A. Vogler, L. Firment, T. Watt, S. Haynie, D. Y. Sogah, *J. Biomed. Mater. Res.* **1993**, *27*, 1463.
[2] A. J. Engler, L. Richert, J. Y. Wong, C. Picart, D. E. Discher, *Surf. Sci.* **2004**, *570*, 142.
[3] K. Anselme, M. Bigerelle, B. Noel, E. Dufresne, D. Judas, A. Iost, P. Hardouin, *J. Biomed. Mater. Res.* **2000**, *49*, 155.
[4] E. A. Vogler, *J. Biomater. Sci. Polym. Ed.* **1999**, *10*, 1015.
[5] N. D. Spencer, M. Textor, in *Materials in Medicine* (Eds: M. O. Speidel, P. Uggowitzer,) ETH, Zürich, Switzerland **1997**, p. 209.
[6] M. S. Lord, C. Modin, M. Foss, M. Duch, A. Simmons, F. S. Pedersen, B. K. Milthorpe, F. Besenbacher, *Biomaterials* **2006**, *27*, 4529.
[7] A. S. G. Curtis, N. Gadegaard, M. J. Dalby, M. O. Riehle, C. D. W. Wilkinson, G. Aitchison, *IEEE Trans. NanoBiosci.* **2004**, *3*, 61.
[8] W.-J. Li, R. Tuli, X. Huang, P. Laquerriere, R. S. Tuan, *Biomaterials* **2005**, *26*, 5158.
[9] R. Kriparamanan, P. Aswath, A. Zhou, L. Tang, K. T. Nguyen, *J. Nanosci. Nanotechnol.* **2006**, *6*, 1905.
[10] H. G. Craighead, C. D. James, A. M. P. Turner, *Curr. Opin. Solid State Mater. Sci.* **2001**, *5*, 177.
[11] O. Zinger, G. Zhao, Z. Schwartz, J. Simpson, M. Wieland, D. Landolt, B. Boyan, *Biomaterials* **2005**, *26*, 1837.
[12] R. G. Flemming, C. J. Murphy, G. A. Abrams, S. L. Goodman, P. F. Nealey, *Biomaterials* **1999**, *20*, 573.
[13] H. Liu, T. J. Webster, *Biomaterials* **2007**, *28*, 354.
[14] M. M. Stevens, J. H. George, *Science* **2005**, *310*, 1135.
[15] A. M. Lipski, C. Jaquiery, H. Choi, D. Eberli, M. Stevens, I. Martin, I.-W. Chen, V. P. Shastri, *Adv. Mater.* **2007**, *19*, 553.
[16] R. Barbucci, D. Pasqui, A. Wirsen, S. Affrossman, A. Curtis, C. Tetta, *J. Mater. Sci. Mater. Med.* **2003**, *14*, 721.
[17] A. Nanci, J. D. Wuest, L. Peru, P. Brunet, V. Sharma, S. Zalzal, M. D. McKee, *J. Biomed. Mater. Res.* **1998**, *40*, 324.
[18] P. T. de Oliveira, A. Nanci, *Biomaterials* **2004**, *25*, 403.
[19] P. T. de Oliveira, S. F. Zalzal, M. M. Beloti, A. L. Rosa, A. Nanci, *J. Biomed. Mater. Res.* **2007**, *80A*, 554.
[20] V. J. Dzau, R. C. Braun-Dullaeus, D. G. Sedding, *Nat. Med.* **2002**, *8*, 1249.
[21] C. Leinenbach, D. Eifler, *Biomaterials* **2006**, *27*, 1200.
[22] A. Thapa, D. C. Miller, T. J. Webster, K. M. Haberstroh, *Biomaterials* **2003**, *24*, 2915.
[23] M. J. Dalby, S. J. Yarwood, M. O. Riehle, H. J. H. Johnstone, S. Affrossman, A. S. G. Curtis, *Exp. Cell Res.* **2002**, *276*, 1.
[24] K. Anselme, M. Bigerelle, *J. Mater. Sci. Mater. Med.* **2006**, *17*, 471.
[25] D. D. Deligianni, N. Katsala, S. Ladas, D. Sotiropoulou, J. Amedee, Y. F. Missirlis, *Biomaterials* **2001**, *22*, 1241.
[26] G. Colon, B. C. Ward, T. J. Webster, *J. Biomed. Mater. Res.* **2006**, *78A*, 595.
[27] E. M. Christenson, K. S. Anseth, J. J. J. P. van den Beucken, C. K. Chan, B. Ercan, J. A. Jansen, C. T. Laurencin, W.-J. Li, R. Murugan, L. S. Nair, S. Ramakrishna, R. S. Tuan, T. J. Webster, A. G. Mikos, *J. Orthop. Res.* **2007**, *25*, 11.
[28] E. K. F. Yim, K. W. Leong, *Nanomedicine* **2005**, *1*, 10.
[29] T. P. Kunzler, T. Drobek, M. Schuler, N. D. Spencer, *Biomaterials* **2007**, *28*, 2175.
[30] N. Sniadecki, R. A. Desai, S. A. Ruiz, C. S. Chen, *Ann. Biomed. Eng.* **2006**, *34*, 59.
[31] P. P. Girard, E. A. Cavalcanti-Adam, R. Kemkemer, J. P. Spatz, *Soft Matter* **2007**, *3*, 307.
[32] K. M. Woo, V. J. Chen, P. X. Ma, *J. Biomed. Mater. Res.* **2003**, *67A*, 531.
[33] K. Rechendorff, M. B. Hovgaard, M. Foss, V. P. Zhdanov, F. Besenbacher, *Langmuir* **2006**, *22*, 10885.
[34] L. Ponsonnet, K. Reybier, N. Jaffrezic, V. Comte, C. Lagneau, M. Lissac, C. Martelet, *Mater. Sci. Eng. C* **2003**, *23*, 551.
[35] K. Irie, S. Zalzal, H. Ozawa, M. D. McKee, A. Nanci, *Anat. Rec.* **1998**, *252*, 554.